JMEPEG (2024) 33:4447–4460
https://doi.org/10.1007/s11665-023-08275-9

1059-9495/$19.00

TECHNICAL ARTICLE

Oxidation Behavior of Silicon-Aluminizing Coating on γ-TiAl Alloy at Different Temperatures

Feng Zhao, Jiang Huang, Xinyu Cui, Jiqiang Wang, and Tianying Xiong

Submitted: 22 February 2023 / Revised: 10 April 2023 / Accepted: 14 April 2023 / Published online: 16 June 2023

In this research, a silicon-aluminizing diffusion coating constituted of homogenous Ti(Al, Si)$_3$ phase was prepared on γ-TiAl alloy using cold spraying Al-40Si (wt.%) alloy coating followed by thermal diffusion treatment. The oxidation behavior of the diffusion coating was tested for 300 h at high temperatures of 900, 950 and 1000 °C. The differences in microstructure evolution at three different temperatures, as well as antioxidant properties of the coating, were investigated. The results showed that the weight gain of the coating after 300-h oxidation at 900, 950 and 1000 °C was sharply reduced to only 1.195, 1.550 and 1.925 mg cm^{-2}, respectively. Although the alumina-based oxide scale formed on the coating became thicker with the increasing oxidation temperature, it had a good adherence to the coating even at 1000 °C. Thus, the coating can significantly improve the oxidation resistance of the γ-TiAl alloy at three temperatures because the generated oxide scale can act as a barrier to prevent the outward diffusion of Ti and the internal diffusion of O. The degradation rate of the coating also increased with the increasing oxidation temperature. Following 300 h of oxidation test at 1000 °C, the homogenous Ti(Al, Si)$_3$ phase in the coating almost entirely degraded. However, the in situ formed Ti$_5$Si$_3$ diffusion layer maintained a good stability at 1000 °C, which can block the further invasion of O to a certain extent.

Keywords γ-TiAl, cold spray, high-temperature oxidation, silicon-aluminizing diffusion coating, Ti_5Si_3

1. Introduction

Intermetallic TiAl-based alloys have been regarded as a promising alternative for Ni-based superalloys applied to the structural components of aerospace, aviation and automobile engines due to their properties such as lightweight, high specific strength, high-temperature resistance, and sufficient high-temperature creep resistance (Ref 1-4). However, one of the major challenges limiting their applications is the poor antioxidant properties at temperatures exceeding 800 °C which is associated with the quick formation of porous titanium oxide or mixed titanium and aluminum oxide films (Ref 5-7). Therefore, it is necessary to protect the materials at elevated temperatures with an antioxidant coating.

A great quantity of studies have been conducted on the surface coatings in an effort to enhance the formation of a protective Al_2O_3 scale while suppressing the TiO_2 formation, which involves aluminide coatings based on $TiAl_3$ and $TiAl_2$ (Ref 8-11), MCrAlY coatings (Ref 12, 13), ceramic and enamel coatings (Ref 14-16). Among them, preparation aluminide coatings with high oxidation resistance seem as one of the most promising methods from the aspects of chemical compatibility, thermal expansion coefficient and cost. However, in the long-term high-temperature environment, the aluminum content of simple aluminide coatings was sharply depleted due to the formation of alumina and the interdiffusion between substrates and coatings, which leads to the degradation and failure of the coatings. Hence, the third element has been added into aluminide coatings to further extend their high-temperature service life, such as PtAl coating (Ref 17, 18), TiAlCr coating (Ref 19, 20) and SiAl coating (Ref 21-25).

According to the research, the introduction of Si in aluminide coatings can enhance the antioxidant properties of the coatings, including extending the service time and increasing the service temperature. As an element with a great affinity to Ti, Si and Ti combine preferentially to form Ti-Si phases, which can reduce Ti activity and hinder its outward diffusion (Ref 21, 24). In addition, Ti-Si phases such as Ti_5Si_3 typically gathered at grain boundaries, acting as diffusion barriers for Al, inhibiting its internal diffusion (Ref 26, 27). In order to better block the internal diffusion of Al, the diffusion barrier should preferably be dense and continuous, which may require a sufficient amount of Si elements to be added into the aluminide coating to generate a continuous Ti-Si phases layer.

Cold spray is a technique of solid-state coating preparation. Therefore, cold sprayed coatings typically have low oxide content, as well as low porosity and stress (Ref 21, 28-30). In prior research work (Ref 31), we prepared a silicon-aluminizing diffusion coating constituted of homogenous Ti(Al, Si)$_3$ phase on γ-TiAl alloy using cold spraying Al-40Si (wt.%) alloy coating followed by thermal diffusion treatment. An in situ Ti_5Si_3 diffusion barrier layer and numerous reticular Ti_5Si_3

Feng Zhao and **Jiang Huang**, Shi-changxu Innovation Center for Advanced Materials, Institute of Metal Research, Chinese Academy of Sciences, Shenyang 110016, People's Republic of China; and School of Materials Science and Engineering, University of Science and Technology of China, Shenyang 110016, People's Republic of China; **Xinyu Cui, Jiqiang Wang,** and **Tianying Xiong**, Shi-changxu Innovation Center for Advanced Materials, Institute of Metal Research, Chinese Academy of Sciences, Shenyang 110016, People's Republic of China. Contact e-mail: jqwang11s@imr.ac.cn.

precipitates were generated in the coating under high-temperature exposure, limiting the mutual diffusion of elements between the γ-TiAl alloy substrate and silicon-aluminizing diffusion coating, consequently improving the long-term antioxidant properties.

In this study, further findings of the oxidation behavior of this silicon-aluminizing coating are provided. Temperatures of 900, 950 and 1000 °C were used to test the coating. The microstructure evolution and oxidation resistance of the coating at different temperatures were investigated. Whether the continuous Ti_5Si_3 layer could be stable at higher temperatures was the main concern. The results obtained within this study would provide evidence in favor of the potential application of the coating in the elevated temperature range.

2. Experimental

The utilized γ-TiAl material was provided by Titanium Alloys Division, Institute of Metal Research, Chinese Academy of Sciences, with a nominal composition of Ti-45Al-2Nb-2Mn (at.%) supplemented with 0.8 vol.% TiB_2. In detail, the γ-TiAl alloy ingot was machined into rectangular specimens with nominal sizes of 15 × 10 × 2 mm. After that, the whole surface was ground to 800 grits with SiC paper, and then, the ultrasonic cleaning was fulfilled in anhydrous alcohol and dried in air. Sandblasting and a second ultrasonic cleaning in alcohol were applied to the specimens that would be coated in order to increase the adherence of the coating to the substrate. The substrate surface roughness before spraying was 1.842 ± 0.146 μm measured by surface roughness measuring instrument (TIME3200, Beijing TIME High Technology Ltd.).

A 30-μm-thick Al-40Si alloy coating was deposited on TiAl substrate by cold spray. The gas temperature, gas pressure and the nozzle-substrate standoff distance were 350 °C, 2 MPa and 20 mm, respectively. The Al-40Si alloy coating was heat-treated at 600 °C for 2 h, and then a silicon-aluminizing coating was formed on the surface of substrate. In particular, all surfaces of the substrate were well coated. Details of the preparation process and microstructure of the coating can be found in our previous work (Ref 31). Afterward, the isothermal oxidation tests were performed at 900, 950 and 1000 °C for 300 h in air in a muffle furnace. To study the microstructure evolution of the silicon-aluminizing diffusion coating, the specimens were removed at the oxidation times of 20, 100 and 300 h. The higher experimental temperature of 1000 °C was applied to determine the antioxidant capacity. During the oxidation tests, the mass variations of all specimens were measured periodically using an electronic balance that had a 0.1 mg precision. To assure reproducibility, each datum presented is the average value of three independent specimens.

SEM–EDS (SSX-550, SHIMADZU and Inspect F50, FEI) was used to examine the microstructure of specimens. XRD (Rigaku D/max2500 pc type equipped with Cu Kα radiation) was used to identify the phases of specimens. The scanning rate was 10°/min, and the scanning step value was 0.02°. Electron probe micro-analysis (EPMA-1610, SHIMADZU) was used to obtain the distribution of elements on the cross section of the coatings.

3. Results

3.1 Isothermal Oxidation Kinetics

The isothermal oxidation kinetics curves of γ-TiAl alloy containing and without the silicon-aluminizing diffusion coating at 900, 950 and 1000 °C for 300 h are shown in Fig. 1. It was that at each of the three oxidation temperatures, the kinetics curves of bare and coated γ-TiAl followed an approximately parabolic law. As shown in Fig. 1(a), the overall weight gains of the γ-TiAl alloys after oxidized at 900, 950 and 1000 °C for 300 h were 3.725, 8.638 and 16.925 mg cm^{-2}, respectively. The oxidation mass gain of the γ-TiAl alloys grew dramatically as the oxidation temperature increased. As also illustrated in Fig. 1(c), the parabolic rate constant (k_p) was doubled at higher temperatures. Obvious change was achieved by the silicon-aluminizing coatings, whose weight gain after 300-h oxidation at 900, 950 and 1000 °C sharply reduced to only 1.195, 1.550 and 1.925 mg cm^{-2}, respectively. The oxidation kinetics of the coating oxidized at 900, 950 and 1000 °C were divided into two phases. The parabolic rate constants of the initial phases were 10.6×10^{-2}, 22.4×10^{-2}, 34.7×10^{-2} mg·$cm^{1/2}$·$h^{1/2}$, respectively, which also increased with temperature. The later rate constants declined sharply indicating much lower oxide growing rate. According to the results of the oxidation kinetics, the silicon-aluminizing coating makes for a marked improvement in high-temperature antioxidant properties of γ-TiAl alloys.

3.2 Oxidation Test at 900 °C

Figure 2 displays the XRD patterns of the uncoated γ-TiAl alloy substrate and the silicon-aluminizing diffusion coating following exposure at 900 °C. It was evident that the oxide film formed on the bare substrate was mainly TiO_2, with a trace quantity of Al_2O_3 mixed in. In addition, nitride phases such as TiN or $AlTi_2N$ were also detected. As seen by the surface morphology in Fig. 3(a), the oxidized bare alloy surface suffered severe spallation. After oxidation, a multilayer oxide film containing Al_2O_3 and TiO_2 was formed, consisting of the outermost TiO_2-enriched layer, the middle Al_2O_3-enriched layer, and the interior loose TiO_2 and Al_2O_3 blend layers, as shown in Fig. 3(b). The bonding strength between this kind of oxide film and the substrate is poor, resulting in readily spalling. Thus, the bare γ-TiAl alloy exhibits inferior oxidation resistance.

The surface morphology of the coating during oxidation (Fig. 3c, e, g) demonstrates that part of TiO_2 is still generated, but the main oxides are made of α-Al_2O_3, containing a tiny quantity of acicular θ-Al_2O_3. The θ-Al_2O_3 decreased as the oxidation time increased, while TiO_2 did not rise considerably, which is in accordance with the XRD result shown in Fig. 2. Although the XRD peaks corresponding to TiO_2 still exist on the oxidized surface of the diffusion coating, it has succeeded in preventing the generation of the loosely mixed layer of TiO_2 and Al_2O_3 or the consecutive TiO_2-enriched layer. The initial phase peak of the diffusion coating was dominated by $TiAl_3$. During oxidation, $TiAl_3$ became weaker, while the peak of Al_2O_3 became increasingly visible, eventually forming a stable Al_2O_3 protective scale. No formation of nitride phases such as TiN or $AlTi_2N$ was detected.

As shown in the cross-sectional morphology of the oxidized coating (Fig. 3d, f, h), a typical four-layer structure has been

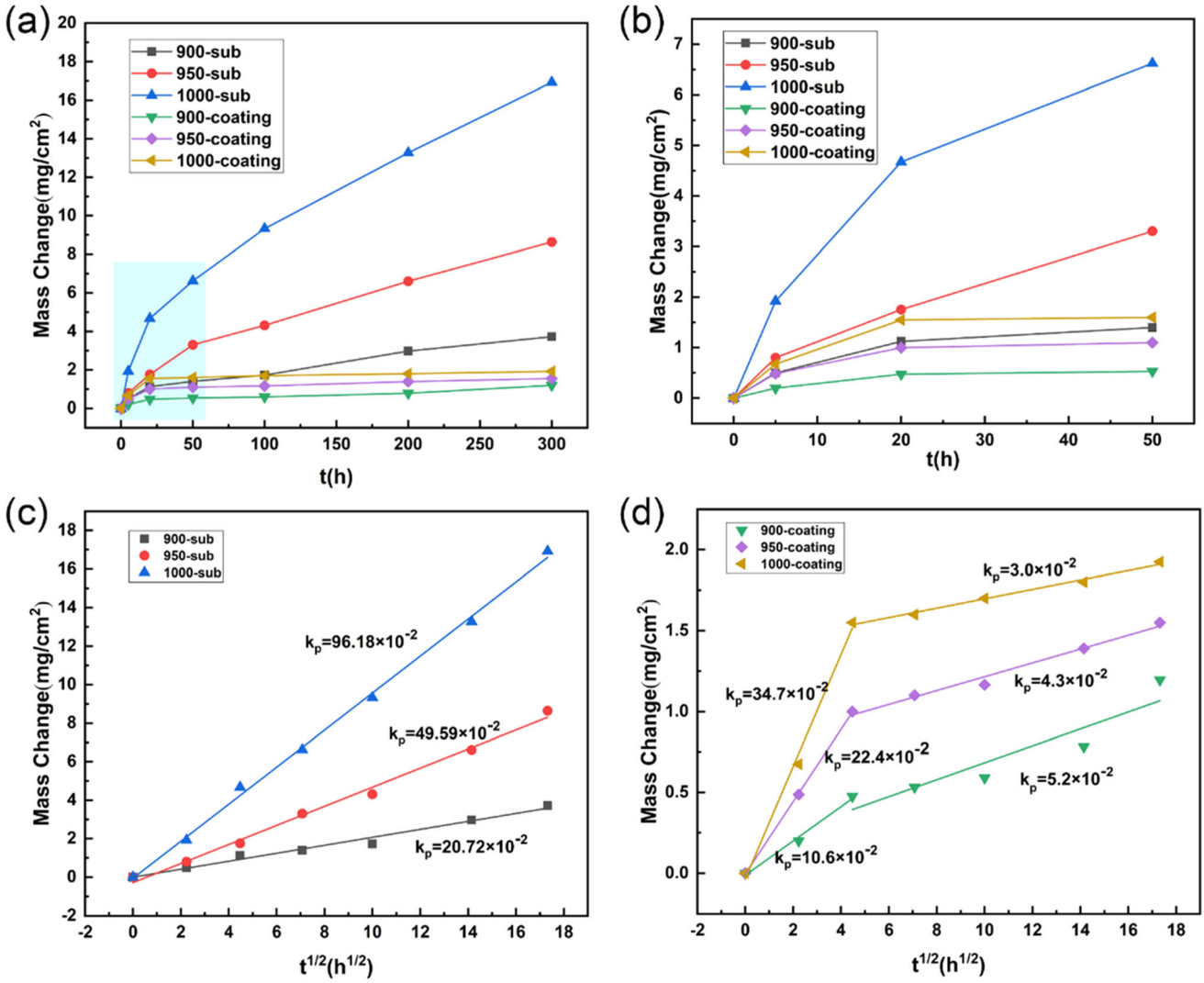

Fig. 1 Isothermal oxidation kinetics curves of γ-TiAl alloy containing and without the silicon-aluminizing diffusion coating at 900, 950 and 1000 °C for 300 h

formed, from top to bottom: (a) a thin oxide layer, (b) a mixing layer composed of Ti(Al, Si)$_3$ phase and reticular structure Si-rich phases, (c) a consecutive Si-rich layer and (d) $TiAl_2$ layer. During the course of oxidation, the thin Al_2O_3-enriched oxide layer thickened over time and had a good adherence to the coating. After oxidation for 300 h, another consecutive thinner Si-rich layer was generated underneath the oxide film, which may be the Ti_5Si_3 identified by the XRD. In addition, a progressive increase in pores and the Si-rich precipitate phases can be observed under prolonged exposure to high temperatures. The thickness of the $TiAl_2$ layer gradually expanded while the Ti(Al, Si)$_3$ mixed layer steadily reduced. Between the mixing layer and the $TiAl_2$ layer, the consecutive Si-rich layer remained essentially unchanged.

Figure 4 illustrates the EPMA elemental distribution diagrams of the diffusion coating following exposure at 900 °C for (a) 20 h, (b) 100 h and (c) 300 h. The element distribution diagram of O reveals that O has intruded into the multihole regions of the coating, but O was scarcely detectable under the continuous Si-rich layer. Another little instruction is that Si-rich phase rarely existed in the $TiAl_2$ layer by comparing the Al, Si and Ti element distribution diagrams. Simultaneously, Ti and Si were overlapping in the same region, that is, the generated Si precipitations are Ti-Si phases.

3.3 Oxidation Test at 950 °C

The surface and cross-sectional morphology of the uncoated γ-TiAl alloy substrate are depicted in Fig. 6(a), (b) following exposure at 950 °C for 300 h. The spallation of the oxides could also be visible from the surface morphology. As the oxidation continues, the surface oxide layer would undergo a back-and-forth cycle of exfoliation-growth-exfoliation-regrowth. Compared to 900 °C, more oxides fell off in the crucible after 300-h oxidation at 950 °C, corresponding to the higher weight gain of γ-TiAl substrate in Fig. 1. A mixed oxide film constituted of Al_2O_3 and TiO_2 was generated indicated by the XRD peaks, which is depicted in Fig. 5 and is plainly apparent in Fig. 6(b). The results revealed that the majority of the oxides on the surface of γ-TiAl substrate were TiO_2, with a little quantity of Al_2O_3, and TiN and $AlTi_2N$ nitride phases were also detected.

Similarly, the coating demonstrated promising oxidation resistance after 300-h oxidation at 950 °C, as evidenced by the

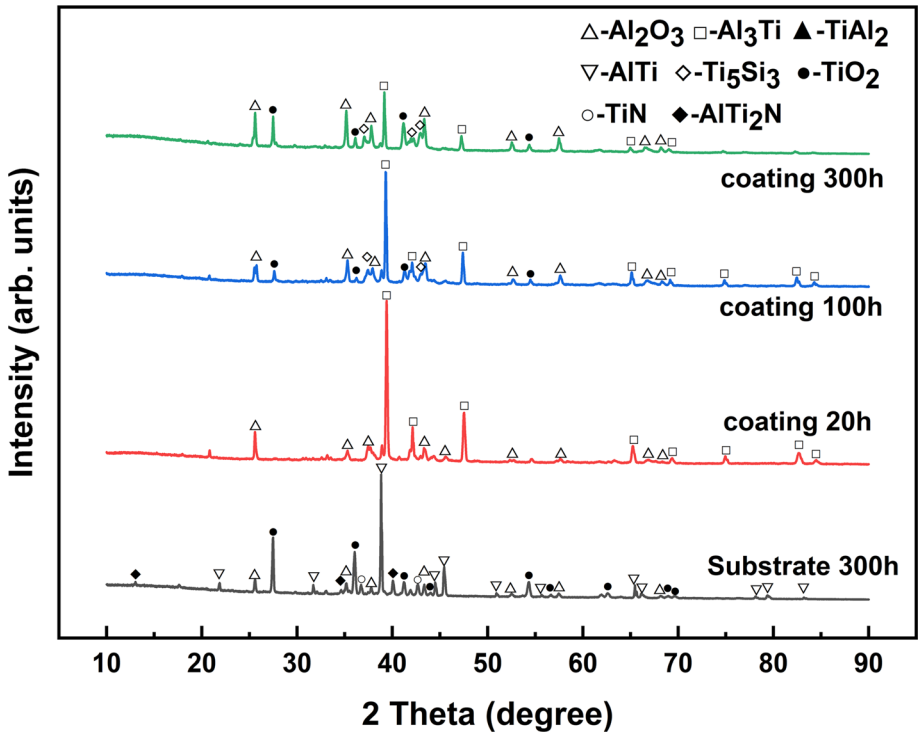

Fig. 2 XRD patterns of the uncoated γ-TiAl alloy and the silicon-aluminizing diffusion coating following exposure at 900 °C

surface and cross-sectional morphology of the coating (Fig. 6c, d). The oxides on the surface were primarily constituted of α-Al_2O_3, but also contained a tiny quantity of residual acicular θ-Al_2O_3 and trace of TiO_2. This result was further confirmed by the XRD pattern of the oxidized coating (Fig. 5). After oxidation for 300 h, the coating was primarily constituted of $TiAl_3$, $TiAl_2$ and Ti_5Si_3 phases. No diffraction peaks of nitride phases were detected by XRD.

As for the cross-sectional morphology of the coating following exposure at 950 °C for 300 h (Fig. 6d), combined with the SEM–EDS results (Fig. 7), it is clear that the coating also exhibits a multilayer structure, including an outmost oxide layer and resulting Ti and Si enriched thin layer, a middle mixed layer composed of $Ti(Al, Si)_3$ phase and reticular structure Si-rich phases, as well as a consecutive Si-rich layer and the inner $TiAl_2$ layer. However, compared to 900 °C, the most noticeable difference was the thickness of the oxide film, which thickened significantly at higher temperature. Specifically, the weight increase in the coating was greater (Fig. 1).

Figure 8 shows the EPMA elemental distribution diagrams of the coating following exposure at 950 °C for 300 h. Analyzing the O element distribution revealed that essentially no O occurred underneath the consecutive Si-rich layer, even at the higher temperature of 950 °C. By comparing the distribution maps of Si, Al and Ti, essentially no Si-rich phases could be found in the $TiAl_2$ layer. Simultaneously, Si and Ti were obviously overlapping in the middle two layers, and the overlapping region was an Al-poor region, which is in accordance with the findings in Fig. 7.

3.4 Oxidation Test at 1000 °C

Figure 9 displays the macroscopic appearance of uncoated γ-TiAl alloy and diffusion coating following exposure at 1000 °C for (a), (d) 20 h, (b), (e) 100 h and (c), (f) 300 h. It could be observed from Fig. 9(a)-(c) that at 1000 °C, the oxide layer on the substrate surface was severely exfoliated, and the exfoliation of oxides increased dramatically as the oxidation period increased. In contrast, only minor spallation of the coating (Fig. 9d-f) occurred.

Figure 11 illustrates the surface and cross-sectional morphology of the uncoated γ-TiAl alloy and diffusion coating following exposure at 1000 °C. The surface morphology of uncoated alloy after oxidation for 300 h revealed severe multilayer peeling (Fig. 11a), which was due to the formation of brittle oxide TiO_2 over time. The multilayer oxide film on the surface of the substrate was also dominated by TiO_2, with a tiny amount of Al_2O_3 mixed in, and the TiN and $AlTi_2N$ nitride phases were also detected, as confirmed by XRD (Fig. 10). In addition, the diffraction peaks of the TiAl phase seem stronger because of the more severe peeling of the oxide film at 1000 °C.

In regard to the surface morphology of the coating, it was primarily formed of α-Al_2O_3, with a minor quantity of acicular θ-Al_2O_3 and TiO_2 from (Fig. 11c, e, g). With the extension of oxidation time, TiO_2 tended to increase and grow up. This result corresponded to the XRD peaks shown in Fig. 10. The main diffraction peaks of Al_2O_3 and Ti_5Si_3 were steadily enhanced over time. Different from 900 to 950 °C, after oxidation at 1000 °C, not only was the $TiAl_2$ phase not detected by XRD, but also the peak of $TiAl_3$ disappeared. This may be caused by an excessively thick surface oxide layer or by this phase degradation at high temperatures.

As for the cross-sectional morphology of the coating following exposure at 1000 °C (Fig. 11d, f, h), comparable phase transitions occurred just like in the oxidation test at 900 °C, so the coating still exhibited a typical four-layer structure. However, the oxide layer was substantially thicker than that at 900 and 950 °C. With the prolongation of oxidation

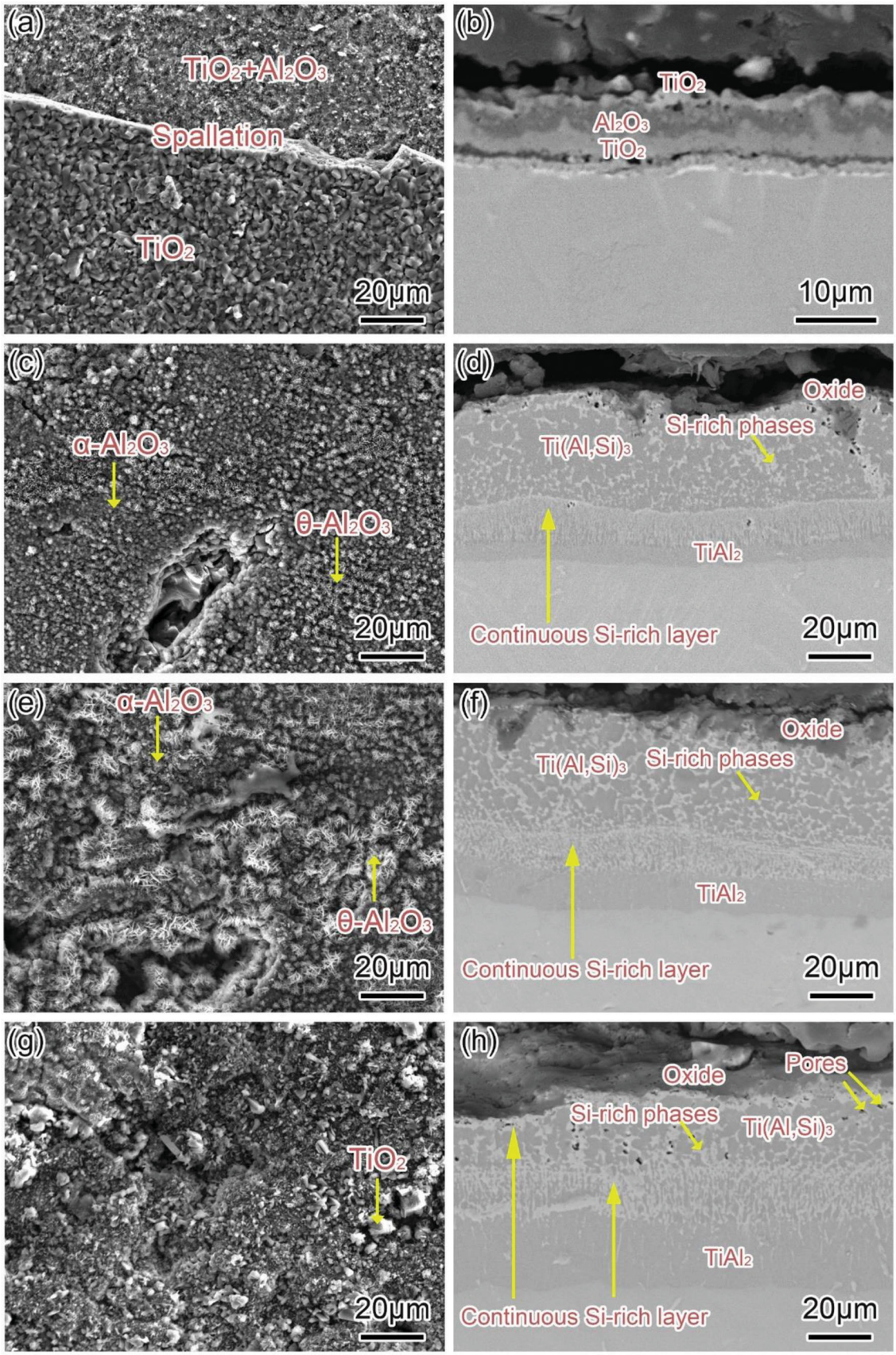

Fig. 3 Surface and cross-sectional morphology of the uncoated alloy for (a, b) 300 h and the silicon-aluminizing diffusion coating following exposure for (c, d) 20 h, (e, f) 100 h, (g, h) 300 h at 900 °C

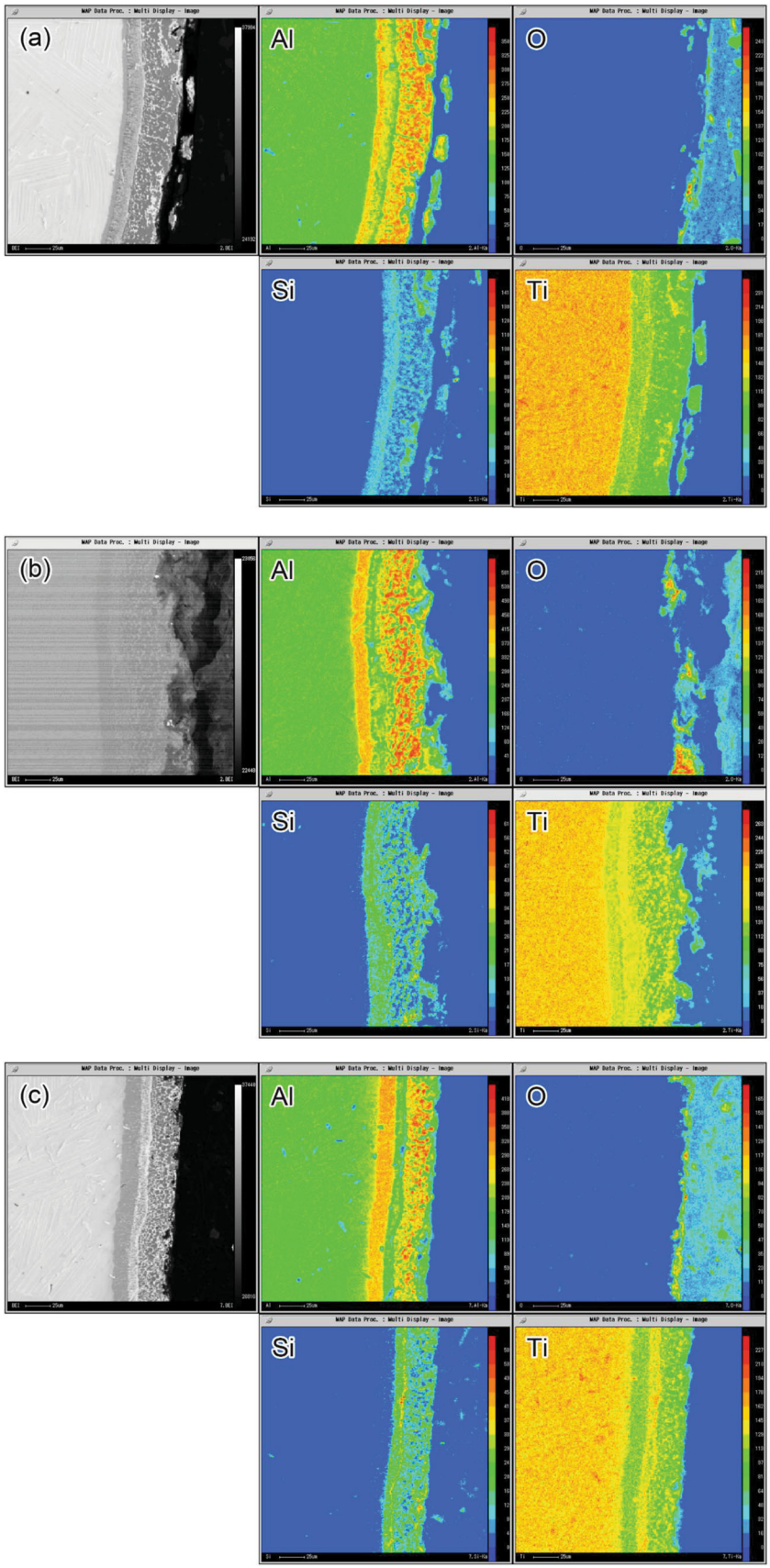

Fig. 4 EPMA elemental distribution diagrams of the cross section of the diffusion coating following exposure at 900 °C for (a) 20 h, (b) 100 h and (c) 300 h

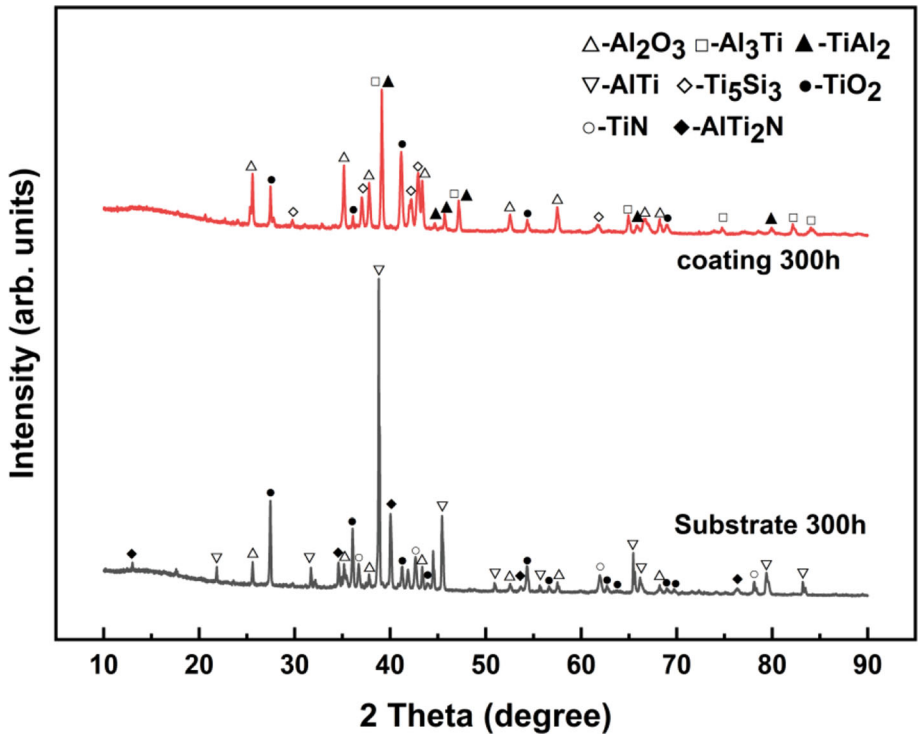

Fig. 5 XRD patterns of the uncoated γ-TiAl alloy and the silicon-aluminizing diffusion coating following exposure at 950 °C

time, the mixed layer constituted of Ti(Al, Si)$_3$ phase and reticular structure Si-rich phases tended to degenerate and become thinner, and Kirkendall pores developed dramatically. It should be noted that the consecutive Si-rich layer still existed stably after 300 h at 1000 °C. The $TiAl_2$ layer showed the phenomenon of first thickening and subsequently thinning.

Figure 12 shows the EPMA elemental distribution diagrams of the diffusion coating following exposure at 1000 °C for (a) 20 h, (b) 100 h and (c) 300 h. Analyzing the O element distribution reveals that even if following exposure at 1000 °C for 300 h, essentially no oxygen emerged underneath the consecutive Si-rich layer. However, it could also be confirmed that the mixed layer constituted of Ti(Al, Si)$_3$ phase and reticular structure Si-rich phases tended to degenerate and thin out. After 300 h of oxidation, the Ti(Al, Si)$_3$ in the coating had nearly completely degraded. The degradation of the inner $TiAl_2$ phases was due to the fact that $TiAl_2$ phases unable existed stably at 1000 °C for a long time, and Al had serious internal diffusion into the substrate.

4. Discussion

4.1 Microstructural Evolution of Silicon-Aluminizing Diffusion Coating during High-Temperature Oxidation

By comparing all research stages of this work and the previous studies (Ref 31) at all testing temperatures, the following microstructural evolution of silicon-aluminizing coating can be concluded, beginning with the Ti(Al, Si)$_3$ following cold spray and heat treatment. Basically, the evolution was similar at every temperature, resulting in similar microstructure, with the main difference being the rate of evolution.

Firstly, based on the results, the initial Ti(Al, Si)$_3$ phase and O_2 chemically reacted to generate a quasi-continuous oxide film at the outermost surface. In addition, significant quantities of Si-rich phases precipitated and aggregated in the Ti(Al, Si)$_3$ grain boundaries (Fig. 3d) and a consecutive Si-rich layer emerged underneath the oxide film, which was an Al-depleted zone (Fig. 3h). It has been reported previously that the maximum Si solubility in $TiAl_3$ is substantially higher than that of $TiAl_2$, 15 at.% in $TiAl_3$ but only about 1.5 at.% in $TiAl_2$ (Ref 32, 33). Therefore, with the degradation of $TiAl_3$, Si in the initial $TiAl_3$ phase would precipitate and aggregate beneath the oxide film because of the decline of Si solubility. Furthermore, Si and Al have enthalpies of dissolution in liquid Ti of −211 and −137 kJ/mol, respectively (Ref 34), suggesting that Si has a significantly better combining ability than Al with Ti, implying that the precipitated Si-rich phases were mainly Ti-Si compounds, which were identified as Ti_5Si_3. From the discussion above, during the oxidation at all testing high temperatures, Al in Ti(Al, Si)$_3$ diffused outward for the Al_2O_3 formation, causing Ti(Al, Si)$_3$ degraded to $TiAl_2$, accompanied by the generation of the Ti_5Si_3 phases. The following expression can be used to summarize the whole oxidation process:

$$\mathrm{Ti(Al,\ Si)_3 + O_2 \rightarrow\ Al_2O_3 +\ Ti_5Si_3 +\ TiAl_2} \qquad \text{(Eq 1)}$$

The similar mechanism applies to the continuous Ti_5Si_3 layer formed in the coating. At high temperatures, due to the difference of element content, the mutual diffusion occurred

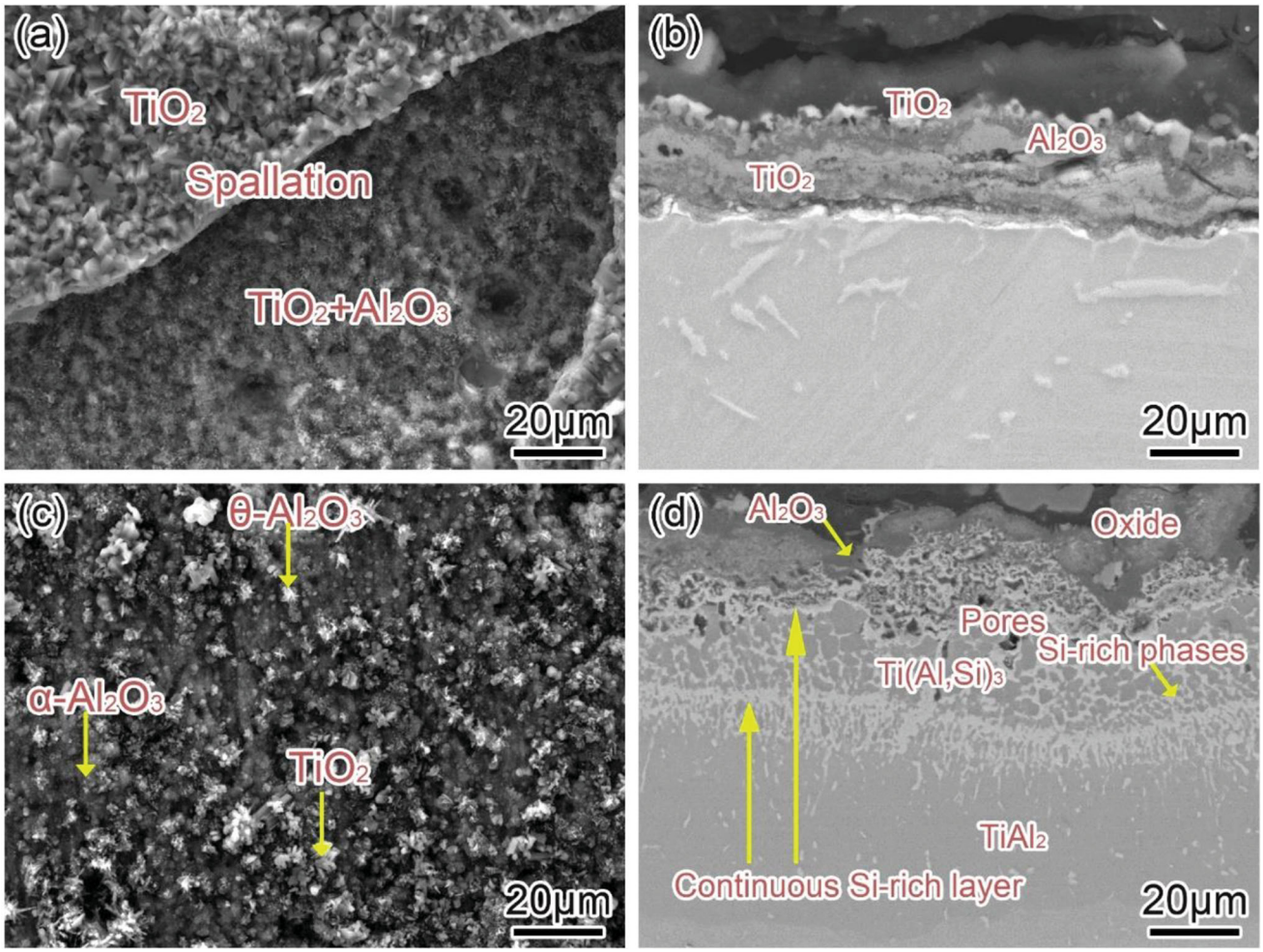

Fig. 6 Surface and cross-sectional morphology of the uncoated alloy for (a, b) 300 h and the silicon-aluminizing diffusion coating following exposure for (c, d) 300 h at 950 °C

between the $Ti(Al, Si)_3$ phase and γ-TiAl substrate, resulting in the generation of a $TiAl_2$ layer. And, as the degradation of $Ti(Al, Si)_3$ caused by Al diffusion into the substrate, a large amount of Si would be liberated from $Ti(Al, Si)_3$ phase on the interface between residual $Ti(Al, Si)_3$ and recently generated $TiAl_2$. Under long-term high-temperature exposure, Si would precipitate and enrich along the interface owing to the low solubility in $TiAl_2$, leading to the generation of the consecutive Si-rich layer verified as Ti_5Si_3. This microstructure evolution process can be represented as follows:

$$Ti(Al,\ Si)_3 + TiAl \rightarrow TiAl_2 + Ti_5Si_3 \qquad \text{(Eq 2)}$$

4.2 Oxidation Behavior and Phase Stability at Different Temperatures

The poor antioxidant properties of γ-TiAl alloy in high-temperature environments owing to the TiO_2 generated by the reaction between internal diffusion of O and outward diffusion of Ti. In contrast, the silicon-aluminizing diffusion coating showed better antioxidant properties at several different temperatures, owing mostly to the generation of the protective oxide films. According to a study, the minimum Al concentration in γ-TiAl alloy required to generate a continuous and protective Al_2O_3 layer was estimated to be 64 at.% (Ref 35). The Al concentration of the diffusion coating was adequate to maintain the generation of a single stable aluminum oxide. It can be confirmed by the XRD patterns (Fig. 2 + 5 + 10) that Al_2O_3 made up the majority of the oxide that has generated on the coating surface.

Furthermore, the introduction of Si showed a beneficial impact on enhancing the formation of the aluminum oxide film on the outermost surface of this diffusion coating. As the affinity between Si and Ti is considerably stronger than that between Al and Ti, the combination of Ti and Si would lower Ti activity, preventing it from diffusing outward to form TiO_2. In other words, this indirectly means an increase in Al activity, which promotes the preferential oxidation of Al. Large amounts of Ti_5Si_3 precipitations, including the reticular structure Ti_5Si_3 phases and the continuous Ti_5Si_3 layer, also play a critical part in the long-term lifetime of the coating at high temperatures. The reticular structure Ti_5Si_3 phases gathered at the grain/phase boundaries may operate as diffusion barriers by preventing Al from diffusing inward to the substrate, hence keeping Al from

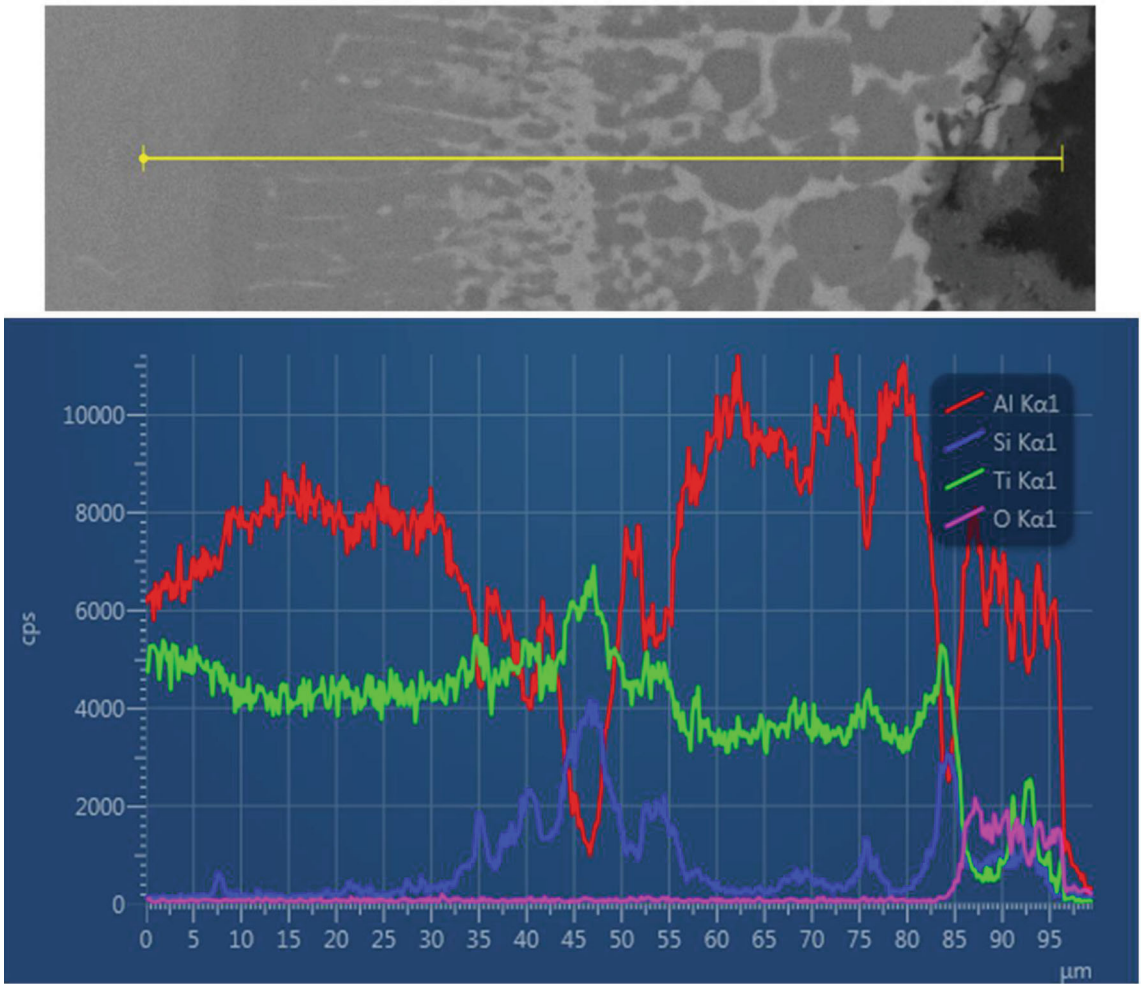

Fig. 7 SEM–EDS line scanning data of the silicon–aluminizing diffusion coating following exposure for 300 h at 950 °C

being depleted from the coating. This phenomenon has been reported in the literature (Ref 21, 26). With respect to the continuous Ti_5Si_3 layer, Bauer et al. (Ref 27) deposited a Ti_5Si_3 interlayer between the 70Al-30Ti (in at.%) layer and the γ-TiAl. It was observed that compared to the single Al-Ti-coated TiAl alloys, coating systems with a Ti_5Si_3 interlayer maintained the Al-rich $TiAl_3$ and $TiAl_2$ phases persistent for around 5-10 times longer. They explained that due to the low solubility of Si in $TiAl_2$ and TiAl, when Ti_5Si_3 was placed next to $TiAl_2$ and TiAl, only a very small quantity of Al could be dissolved in the Ti_5Si_3 interlayer, resulting in a minimum lattice diffusion flux when bulk diffusion of Al through Ti_5Si_3 occurred. Therefore, the in situ continuous Ti_5Si_3 layer can be used as a diffusion barrier layer to better prevent Al from diffusing inward to the substrate, reduce the degradation rate of the diffusion coating, and improve its long-term antioxidant properties.

On the other hand, essentially no oxygen emerged under the continuous Ti_5Si_3 layer (Fig. 12c), and it has been reported that O diffusivity in Ti_5Si_3 is virtually identical to that of Al_2O_3, and much lower than that of SiO_2, Cr_2O_3 and TiO_2 (Ref 36). As a result, the Ti_5Si_3 layer could also be regarded as a barrier layer preventing O penetration into the γ-TiAl alloy substrate.

The difference with respect to the lower test temperature is that the phase transition rate is quicker because of the higher temperature resulting in quicker mutual diffusion. From 900 to 1000 °C, the amount of Kirkendall pores caused by the interdiffusion increased significantly, and the oxide layer thickened greatly. In addition, the degradation rate of $Ti(Al, Si)_3$ was obviously faster. It is widely acknowledged that diffusion occurs more quickly at higher temperatures. As the temperature raising, metal and oxygen will diffuse through the oxide film at a faster rate, considerably increasing the rate of oxidation. And, at higher temperatures, such as 1000 °C, the Kirkendall diffusion of the Ti and Al caused a significant number of vacancies, which merged at a faster rate, resulting in a porous film in the coating. Subsequent exposure at high temperature, the remaining $Ti(Al, Si)_3$ beneath the oxide film would continue to oxidized due to the invasion of O through the not dense oxide film. In consequence, the thickness of the oxide film was increased greatly. On the other hand, with an increase in temperature, interdiffusion rate between the $TiAl_3$ and $TiAl_2$ layers in the coating and the substrate will be faster, resulting in not only complete degradation of $TiAl_3$, but also serious degradation of $TiAl_2$ phase.

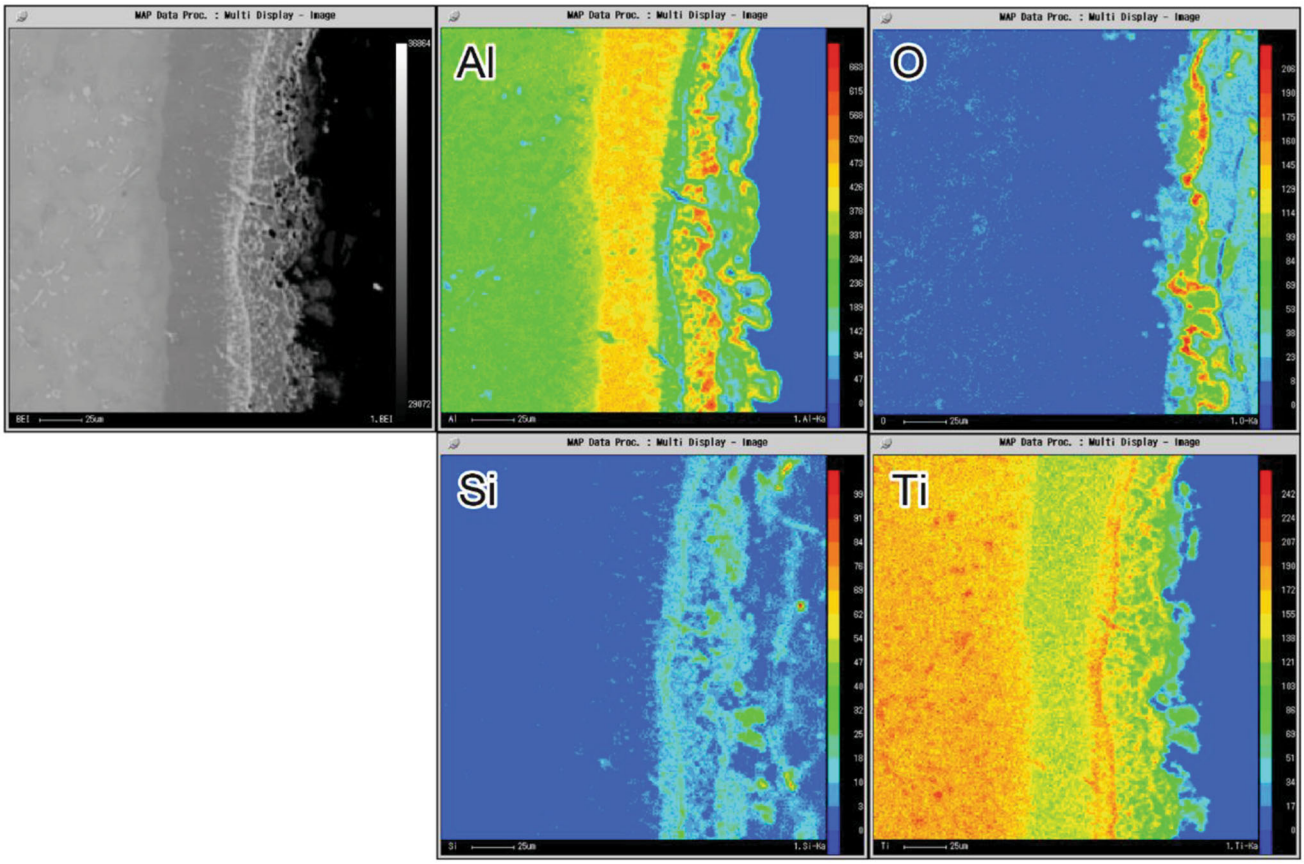

Fig. 8 EPMA elemental distribution diagrams of the cross section of the diffusion coating following exposure at 950 °C for 300 h

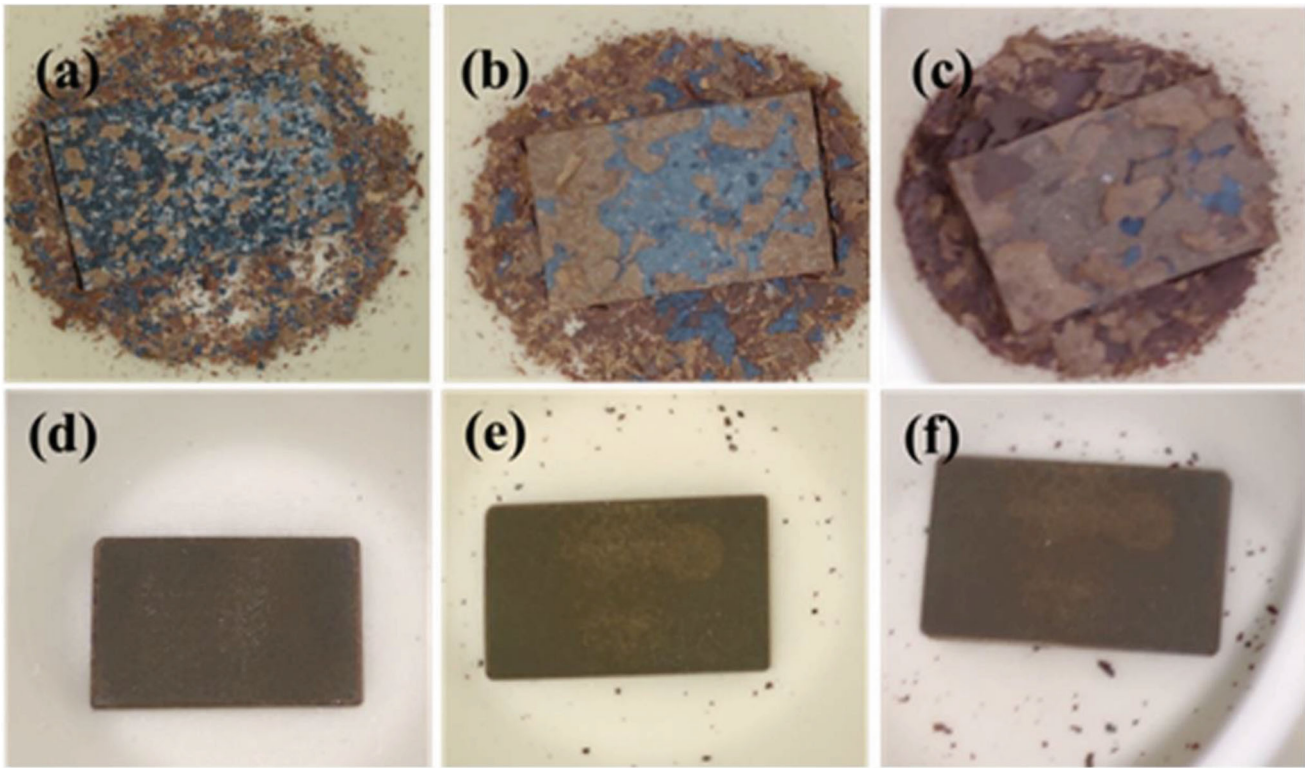

Fig. 9 Macroscopic appearance of the uncoated γ-TiAl alloy (a-c) and the silicon-aluminizing diffusion coating (d-f) following exposure at 1000 °C for (a, d) 20 h, (b, e) 100 h, (c, f) 300 h

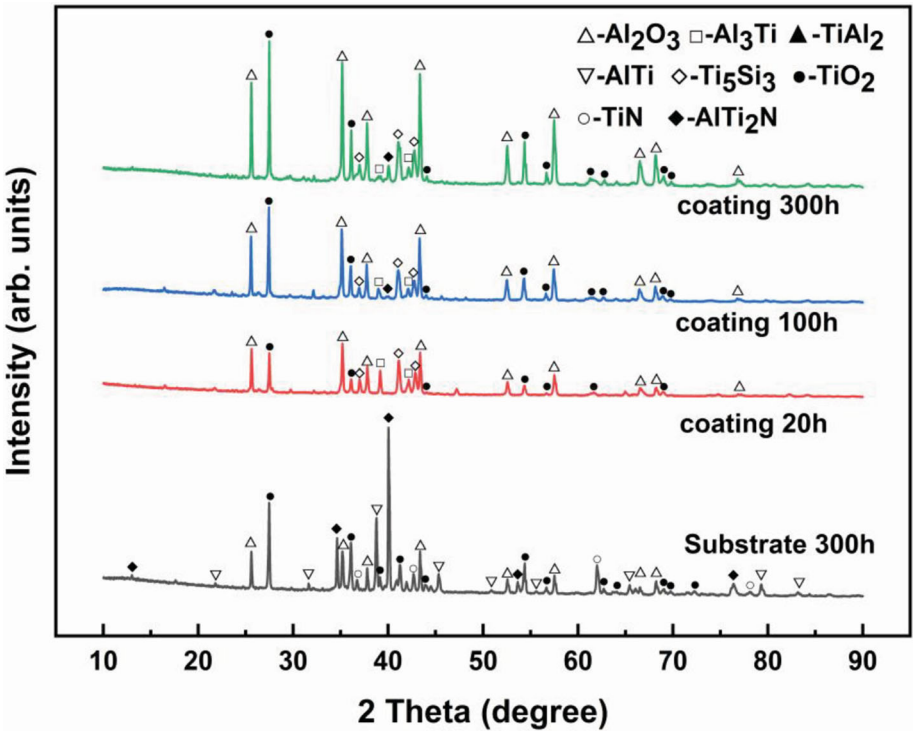

Fig. 10 XRD patterns of the uncoated γ-TiAl alloy and the silicon-aluminizing diffusion coating following exposure at 1000 °C

Another issue that has to be discussed is the long-term stability of the phases of the coating at elevated temperatures, mainly the Ti_5Si_3 phases in this case, including the continuous Ti_5Si_3 layer as well as the reticular structure Ti_5Si_3 phases. During long-term oxidation, the Ti_5Si_3 phases still existed stably and nearly unchanged with the initial state. Even at 1000 °C, the continuous Ti_5Si_3 diffusion barrier formed inside the coating did not degrade and maintained remarkable stability (Fig. 11h), indicating that Al could still be prevented from diffusing inward. Consequently, it is possible to slow down the degradation rate and ensure the long service life of the coating. This phenomenon is also mainly caused by the reduced Si solubility in the TiAl and the $TiAl_2$ phases formed by degradation. In addition, the reticular Ti_5Si_3 phases in the coating were basically stable, with only a tiny percentage degraded (Fig. 11h), which was speculated to be oxidation. In the previous study (Ref 24, 37), the oxidation of Ti_5Si_3 at high temperature would cause the formation of TiO_2 and amorphous SiO_2. The clearances between the TiO_2 grains would be sealed by amorphous SiO_2 to generate a dense structure (Ref 38, 39), which will restrain the inward diffusion of O and thus inhibit the growth of TiO_2. Therefore, even if the $TiAl_3$ and $TiAl_2$ phases are entirely degraded, the remaining reticular Ti_5Si_3 phases in the coating could generate the dense oxide film to prevent the further invasion of O.

5. Conclusions

The antioxidant properties of a silicon-aluminizing diffusion coating on γ-TiAl were examined after isothermal oxidation test at 900, 950, 1000 °C for 300 h, and the differences in microstructure evolution at three different temperatures were evaluated. The conclusions are as followings:

(1) The diffusion coating could effectively enhance the high-temperature antioxidant properties of γ-TiAl at 900, 950 and 1000 °C. This is mainly due to the generated aluminum oxide layer, which functions as a barrier to prevent the outward diffusion of Ti and the internal diffusion of O.

(2) During the exposure at elevated temperatures, the silicon-aluminizing formed the comparable microstructure: (a) a thin oxide layer, (b) a mixed layer composed of $Ti(Al, Si)_3$ phase and reticular structure Ti_5Si_3 phases, (c) a consecutive Ti_5Si_3 layer and (d) $TiAl_2$ layer. With temperature increasing, the thickness of oxide film was increased, as did the degradation rate of $Ti(Al, Si)_3$ and $TiAl_2$.

(3) Following 300 h of oxidation test at 1000 °C, the continuous Ti_5Si_3 layer in the coating does not degrade and maintains a good stability. Even if the $Ti(Al, Si)_3$ and $TiAl_2$ phases are nearly completely degraded, Ti_5Si_3 phases can block the further invasion of O to a certain extent.

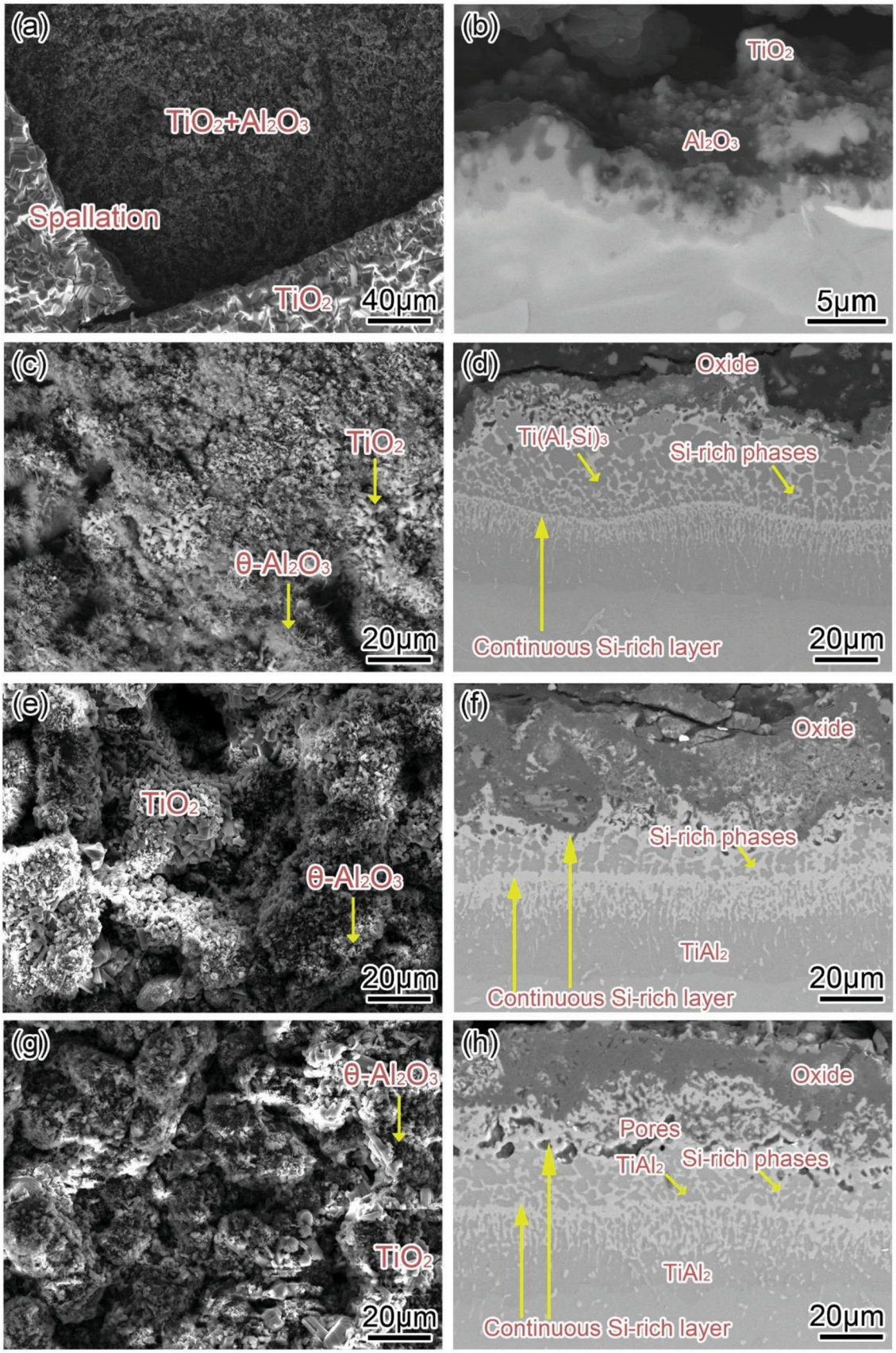

Fig. 11 Surface and cross-sectional morphology of the uncoated alloy for (a, b) 300 h and the silicon-aluminizing diffusion coating following exposure for (c, d) 20 h, (e, f) 100 h, (g, h) 300 h at 1000 °C

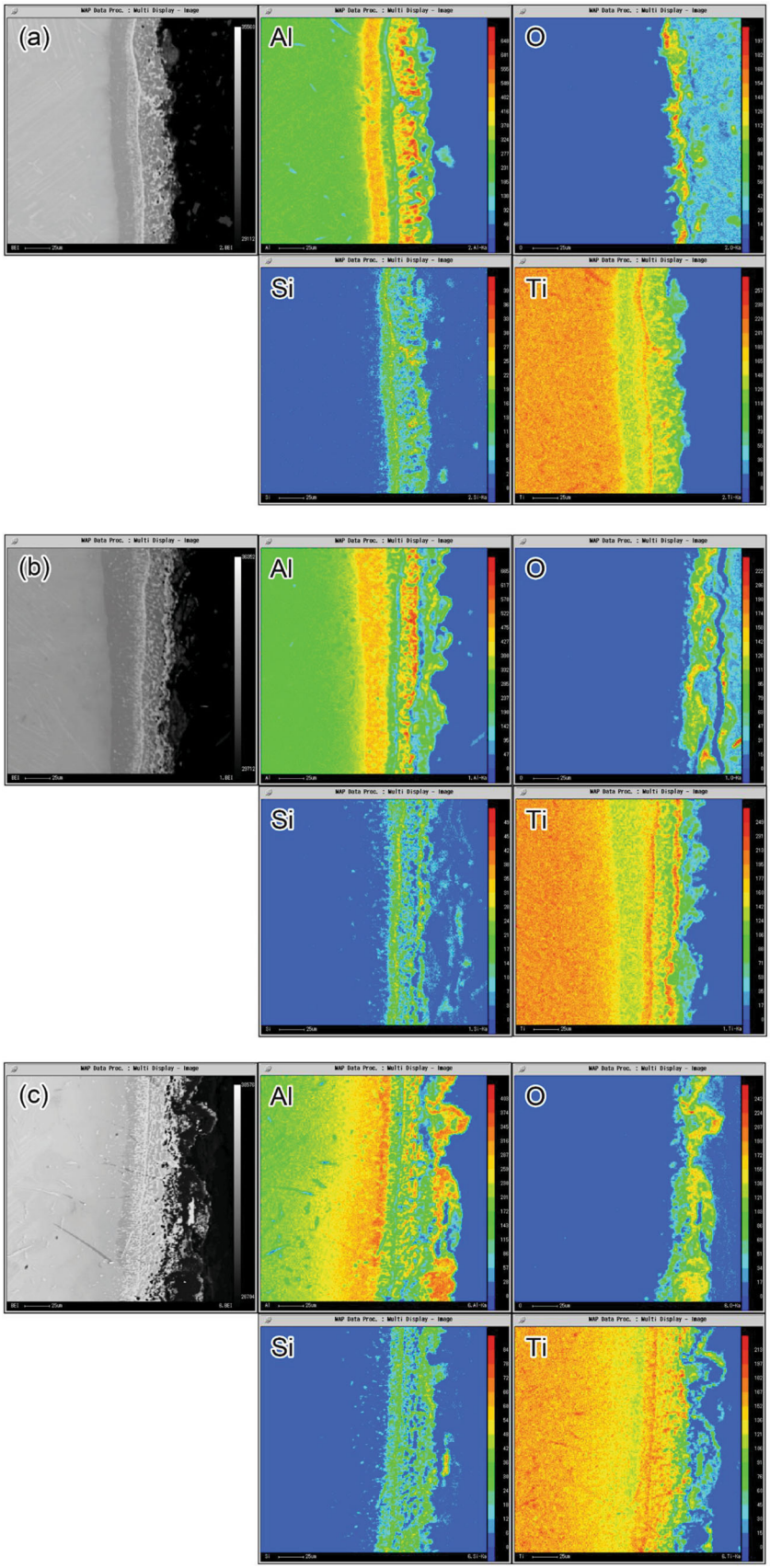

Fig. 12 EPMA elemental distribution diagrams of the cross section of the diffusion coating following exposure at 1000 °C (a) for 20 h, (b) 100 h and (c) 300 h

Acknowledgments

This work was supported by the National Natural Science Foundation of China (Grant No. 52271078 and 51801217) and Key Research Program of the Chinese Academy of Sciences (Grant No. ZDRW-CN-2021-2-2).

References

1. H. Clemens and H. Kestler, Processing and Applications of Intermetallic γ-TiAl-Based Alloys, *Adv. Eng. Mater.*, 2000, **2**, p 551–570.
2. F. Appel, U. Brossmann, U. Christoph, S. Eggert, P. Janschek, U. Lorenz, J. Mullauer, M. Oehring, and J.D.H. Paul, Recent Progress in the Development of Gamma Titanium Aluminide Alloys, *Adv. Eng. Mater.*, 2000, **2**, p 699–720.
3. K. Kothari, R. Radhakrishnan, and N.M. Wereley, Advances in Gamma Titanium Aluminides and Their Manufacturing Techniques, *Prog. Aerosp. Sci*, 2012, **55**, p 1–16.
4. H. Clemens and S. Mayer, Design, Processing, Microstructure, Properties, and Applications of Advanced Intermetallic TiAl Alloys, *Adv. Eng. Mater.*, 2013, **15**, p 191–215.
5. S. Becker, A. Rahmel, M. Schorr, and M. Schutze, Mechanism of Isothermal Oxidation of the Intermetallic TiAl and of TiAl Alloys, *Oxid. Met.*, 1992, **38**, p 425–464.
6. A. Rahmel, W.J. Quadakkers, and M. Schutze, Fundamentals of TiAl Oxidation–A Critical Review, *Werkst. Korros.*, 1995, **46**, p 271–285.
7. D.W. McKee and S.C. Huang, The Oxidation Behavior of Gamma-Titanium Aluminide Alloys under Thermal Cycling Conditions, *Corros. Sci.*, 1992, **33**, p 1899–1914.
8. L.Y. Kong, J.Z. Qi, B. Lu, R. Yang, X.Y. Cui, T.F. Li, and T.Y. Xiong, Oxidation Resistance of $TiAl_3$-Al Composite Coating on Orthorhombic Ti_2AlNb Based Alloy, *Surf. Coat. Technol.*, 2010, **204**, p 2262–2267.
9. T. Sasaki, T. Yagi, T. Watanabe, and A. Yanagisawa, Aluminizing of TiAl-Based Alloy Using Thermal Spray Coating, *Surf. Coat. Technol.*, 2011, **205**, p 3900–3904.
10. Z.Y. Liu and G.D. Wang, Improvement of Oxidation Resistance of γ-TiAl At 800 and 900 °C in Air by $TiAl_2$ Coatings, *Mater. Sci. Eng. A*, 2005, **397**, p 50–57.
11. M.S. Chu and S.K. Wu, The Improvement of High Temperature Oxidation of Ti-50Al by Sputtering Al Film and Subsequent Interdiffusion Treatment, *Acta Mater.*, 2003, **51**, p 3109–3120.
12. Q.M. Wang, K. Zhang, J. Gong, Y.Y. Cui, C. Sun, and L.S. Wen, NiCoCrAlY Coatings with and without an Al_2O_3/Al Interlayer on an Orthorhombic Ti_2AlNb-Based Alloy: Oxidation and Interdiffusion Behaviors, *Acta Mater.*, 2007, **55**, p 1427–1439.
13. Z.L. Tang, F.H. Wang, and W.T. Wu, Effect of MCrAlY Overlay Coatings on Oxidation Resistance of TiAl Intermetallics, *Surf. Coat. Technol.*, 1998, **99**, p 248–252.
14. Z.L. Tang, F.H. Wang, and W.T. Wu, Effect of Al_2O_3 and Enamel Coatings on 900 °C Oxidation and Hot Corrosion Behaviors of Gamma-TiAl, *Mater. Sci. Eng. A*, 2000, **276**, p 70–75.
15. W.B. Li, S.L. Zhu, M.H. Chen, C. Wang, and F.H. Wang, Development of an Oxidation Resistant Glass-Ceramic Composite Coating on Ti-47Al-2Cr-2Nb Alloy, *Appl. Surf. Sci.*, 2014, **292**, p 583–590.
16. S. Sarkar, S. Datta, S. Das, and D. Basu, Oxidation Protection of Gamma-Titanium Aluminide Using Glass-Ceramic Coatings, *Surf. Coat. Technol.*, 2009, **203**, p 1797–1805.
17. A. Ebach-Stahl and M. Fröhlich, Lifetime Study of Sputtered PtAl Coating on γ-TiAl with and without TBC Topcoat at High Temperatures, *Surf. Coat. Technol.*, 2019, **377**, p 124907.
18. A. Ebach-Stahl and M. Frohlich, Oxidation Study of Pt-Al Based Coatings on γ-TiAl at 950 °C, *Surf. Coat. Technol.*, 2016, **287**, p 20–24.
19. R. Swadźba and P.-P. Bauer, Microstructure Formation and High Temperature Oxidation Behavior of Ti-Al-Cr-Y-Si Coatings on TiAl, *Appl. Surf. Sci.*, 2021, **562**, p 150191.
20. H.G. Jung, D.J. Jung, and K.Y. Kim, Effect of Cr Addition on the Properties of Aluminide Coating Layers Formed on TiAl Alloys, *Surf. Coat. Technol.*, 2002, **154**, p 75–81.
21. J.Q. Wang, L.Y. Kong, J. Wu, T.F. Li, and T.Y. Xiong, Microstructure Evolution and Oxidation Resistance of Silicon-Aluminizing Coating on γ-TiAl Alloy, *Appl. Surf. Sci.*, 2015, **356**, p 827–836.
22. G. Moskal, D. Migas, B. Mendala, P. Kałamarz, M. Mikuśkiewicz, A. Iqbal, S. Jucha, and M. Góral, The Si Influence on the Microstructure and Oxidation Resistance of Ti-Al Slurry Coatings on Ti-48Al-2Cr-2Nb Alloy, *Mater. Res. Bull.*, 2021, **141**, p 111336.
23. K. Bobzin, T. Brögelmann, C. Kalscheuer, and T. Liang, Al-Si and Al-Si-Y Coatings Deposited by HS-PVD for the Oxidation Protection of γ-TiAl, *Surf. Coat. Technol.*, 2018, **350**, p 587–595.
24. H.P. Xiong, W. Mao, Y.H. Xie, W.L. Ma, Y.F. Chen, X.H. Li, J.P. Li, and Y.Y. Cheng, Liquid-Phase Siliconizing by Al-Si Alloys at the Surface of a TiAl-Based Alloy and Improvement in Oxidation Resistance, *Acta Mater.*, 2004, **52**, p 2605–2620.
25. R. Swadźba, L. Swadźba, B. Mendala, P.-P. Bauer, N. Laska, and U. Schulz, Microstructure and Cyclic Oxidation Resistance of Si-Aluminide Coatings on γ-TiAl at 850 °C, *Surf. Coat. Technol.*, 2020, **403**, p 123361.
26. P.P. Bauer, N. Laska, and R. Swadzba, Increasing the Oxidation Resistance of γ-TiAl by Applying a Magnetron Sputtered Aluminum and Silicon Based Coating, *Intermetallics (Barking)*, 2021, **133**, p 107177.
27. P.P. Bauer, R. Swadzba, L. Klamann, and N. Laska, Aluminum Diffusion Inhibiting Properties of Ti_5Si_3 at 900 °C and its Beneficial Properties on Al-Rich Oxidation Protective Coatings on γ-TiAl, *Corros. Sci.*, 2022, **201**, p 110265.
28. N. Kaur, M. Kumar, S.K. Sharma, D.Y. Kim, S. Kumar, N.M. Chavan, S.V. Joshi, N. Singh, and H. Singh, Study of Mechanical Properties and High Temperature Oxidation Behavior of a Novel Cold-Spray Ni-20Cr Coating on Boiler Steels, *Appl. Surf. Sci.*, 2015, **328**, p 13–25.
29. H. Assadi, F. Gartner, T. Stoltenhoff, and H. Kreye, Bonding Mechanism in Cold Gas Spraying, *Acta Mater.*, 2003, **51**, p 4379–4394.
30. J.Q. Wang, L.Y. Kong, T.F. Li, and T.Y. Xiong, A Novel $TiAl_3/Al_2O_3$ Composite Coating on γ-TiAl Alloy and Evaluating the Oxidation Performance, *Appl. Surf. Sci.*, 2016, **361**, p 90–94.
31. J. Huang, F. Zhao, X.Y. Cui, J.Q. Wang, and T.Y. Xiong, Long-Term Oxidation Behavior of Silicon-Aluminizing Coating with an In-situ Formed Ti_5Si_3 Diffusion Barrier on γ-TiAl Alloy, *Appl. Surf. Sci.*, 2022, **582**, p 152444.
32. O. Dezellus, B. Gardiola, J. Andrieux, M. Lomello-Tafin, and J.C. Viala, On the Liquid/Solid Phase Equilibria in the Al-Rich Corner of the Al-Si-Ti Ternary System, *J. Phase Equilibria Diffus.*, 2014, **35**, p 137–145.
33. S.P. Gupta, Intermetallic Compounds in Diffusion Couples of Ti with an Al-Si Eutectic Alloy, *Mater. Charact.*, 2002, **49**, p 321–330.
34. A.R. Miedema, F.R. Deboer, and R. Boom, Model Predictions for the Enthalpy of Formation of Transition Metal Alloys, *Calphad*, 1977, **1**, p 341–359.
35. K.L. Luthra, Stability of Protective Oxide-Films on Ti-Base Alloys, *Oxid. Met.*, 1991, **36**, p 475–490.
36. A.V. Bakulin, L.S. Chumakova and S.E. Kulkova, Oxygen Absorption and Diffusion in Ti_5Si_3, *Intermetallics (Barking)*, 2022, **146**, p 107587.
37. J.J. Williams and M. Akinc, Oxidation Resistance of Ti5Si3 and $Ti_5Si_3Z_x$ at 1000 °C (Z = C, N, or O), *Oxid. Met.*, 2002, **58**, p 57–71.
38. Q. Lu, Y.Z. Lv, C. Zhang, H.B. Zhang, W. Chen, Z.Y. Xu, P.Z. Feng, and J.L. Fan, Highly Oxidation-Resistant Ti-Mo Alloy with Two-Scale Network Ti_5Si_3 Reinforcement, *J. Mater. Sci. Technol.*, 2022, **110**, p 24–34.
39. Q. Lu, Y.A. Hao, Y.Y. Wang, P.Z. Feng, and J.L. Fan, Microstructural Evolution and High-Temperature Oxidation Mechanisms of a Ti-Mo-Si Composite, *Corros. Sci.*, 2019, **161**, p 108180.